Electronic Supplementary Material (ESI) for ChemComm.

Supporting Information

Stimuli-Responsive Flexible Lewis Pair-Modified Nanoparticles for Fluorescence Imaging

*Nicole E. Arsenault, Kathleen T. Downey, Michael O. Wolf**

Table of Contents

Synthesis of new compounds

Synthesis procedures involving air or moisture-sensitive reagents were carried out using standard Schlenk techniques under inert N_2 atmosphere. Dry dichloromethane (DCM) was obtained from an Inert PureSolv MD5 Solvent Purification System (SPS). N-hydroxysuccinimide, N-(3-dimethylaminopropyl)-N'-ethylcarbodiimide hydrochloride (EDC•HCl), CuI, and ascorbic acid were purchased from Sigma Aldrich and used as received. Azide-functionalized carboxylic acid[1] and **alkyne-FlexLP**[2] were synthesized according to previous literature methods.

NHS-N_3

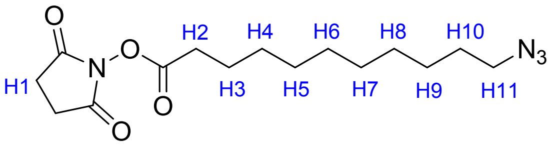

Azide-functionalized carboxylic acid (330 mg, 1.37 mmol), N-hydroxysuccinimide (190 mg, 1.65 mmol), and EDC•HCl (430 mg, 2.25 mmol) were added to a 20 mL vial equipped with stir bar, and purged with N_2. Dry DCM (8 mL) was added to the reaction by syringe to dissolve the compounds, and the reaction stirred overnight under inert atmosphere at room temperature. The reaction was extracted with EtOAc and washed with H_2O and brine, and the organic layer dried over Na_2SO_4. The organic layer was filtered to remove Na_2SO_4, and the product collected by removal of solvent under reduced pressure. The product was collected as a white solid. Yield: 440 mg, 99%. ^1H NMR ($CDCl_3$, 400 MHz): δ 1.24-1.42 (m, 12H, H4-H9), 1.59 (quintuplet, 2H, H3/H10), 1.74 (quintuplet, 2H, H3/H10), 2.60 (t, 2H, H2/H11), 2.83 (s, 4H, H1), 3.25 (t, 2H, H2/H11). $^{13}C\{^1H\}$ ($CDCl_3$,100 MHz): δ 24.7 (CH_2), 25.7 (CH_2), 26.8 (CH_2), 28.9 (CH_2), 29.0 (CH_2), 29.14 (CH_2), 29.2 (CH_2), 29.3 (CH_2), 29.5 (CH_2), 31.1 (CH_2), 51.6 (CH_2), 168.8 (C_4), 169.4 (C_4). HRMS (EI-MS) *m/z:* $[M + Na]^+$ calcd for $C_{15}H_{24}N_4O_4Na$: 347.1695; found 347.1705.

NHS-FlexLP

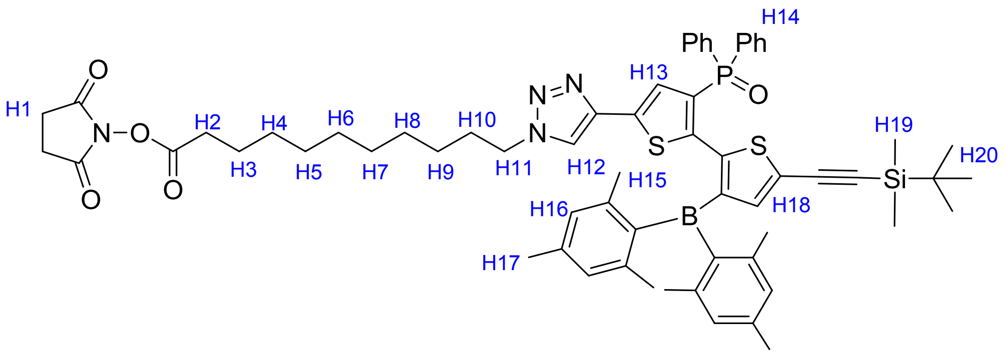

NHS-N_3 (103 mg, 0.32 mmol), **alkyne-FlexLP** (135 mg, 0.17 mmol), CuI (15 mg, 0.08 mmol), and ascorbic acid (3 mg, 0.02 mmol) were added to a 50 mL round bottom flask equipped with Schlenk arm and stir bar, and purged with N_2. THF (20 mL, degassed with N_2 for 1 hr) was added by syringe, and the reaction stirred for 2 days under inert atmosphere at room temperature. The THF was removed under reduced pressure, the residue extracted using EtOAc and washed with H_2O and brine, and the organic layer dried using $MgSO_4$. The organic layer was filtered and EtOAc solvent removed under reduced pressure. The crude product was purified by silica gel column chromatography using EtOAc/hexane (1:1 v/v), and the second major spot collected to afford a yellow solid. Yield: 122 mg, 70%. ^{1}H NMR ($CDCl_3$, 400 MHz): δ 0.14 (s, 6H, H19), 0.95 (s, 9H, H20), 1.30-1.39 (m, 13H, H3-H9), 1.73 (m, 3H, H3/H10), 1.88 (s, 12H, H15), 2.16 (s, 6H, H17), 2.59 (t, J = Hz, 2H, H2), 2.83 (s, 4H, H1), 4.33 (t, J = Hz, 2H, H11), 6.48 (s, 4H, H16), 6.88-6.89 (m, 2H, H13 + H18), 7.38 (m, 8H, H14), 7.54 (m, 3H, H14 + H12). $^{13}C\{^1H\}$ ($CDCl_3$,100 MHz): δ -4.5 (CH_3), 16.9 (C_4), 21.0 (CH_3), 24.5 (CH_3), 24.7 (CH_2), 25.7 (CH_2), 26.4 (CH_3), 26.6 (CH_2), 28.8 (CH_2), 29.0 (CH_2), 29.1 (CH_2), 29.3 (CH_2), 29.3 (CH_2), 30.4 (CH_2), 31.1 (CH_2), 50.7 (CH_2), 98.7 (C_4), 98.9 (C_4), 119.6 (CH), 122.4 (C_4), 123.9 (C_4), 127.6 (C_4), 127.8 (C_4), 128.6 (d, J = 13 Hz, CH), 128.9 (CH), 129.6 (d, J = 113 Hz, C_4), 132.3 (d, J = 17 Hz, CH), 132.6 (d, J = 11 Hz, CH), 132.7 (d, J = 3 Hz, CH), 135.5 (C_4), 137.2 (C_4), 141.8 (CH), 141.9 (d, J = 166 Hz, C_4), 150.3 (C_4), 151.8 (C_4), 160.0 (C_4), 168.8 (C_4), 169.3 (C_4). $^{31}P\{1H\}$ NMR ($CDCl_3$, 162 MHz): δ 33.0. HRMS (EI-MS) *m/z:* $[M + H]^+$ calcd for $C_{63}H_{75}O_5S_2N_4PSi^{11}B$: 1101.4779; found 1101.4774. Elemental analysis calcd for $C_{63}H_{74}O_5S_2N_4PSi^{11}B$: C 68.71, H 6.77, N 5.09, found: C 68.58, H 6.98, N 4.98.

Synthesis of nanoparticles

NP-FlexLP synthesis with varying weight percentage of **NHS-FlexLP** to **NP-NH₂** were synthesized in the following manner.

Amine-functionalized silica nanoparticles (synthesized according to previous literature methods)[3] (**NP-NH₂**, 40 mg) and the appropriate weight percentage of **NHS-FlexLP** (1.2 mg, 2.0 mg, and 4.0 mg for **3%** (**NP-FlexLP-3**), **5%** (**NP-FlexLP-5**), and **10%** (**NP-FlexLP-10**) samples respectively) were added to a 100 mL round bottom flask with a stir bar, and 40 mL of EtOH was added. The reaction stirred in the dark for 16 hours at room temperature in air. The reaction was centrifuged at 2790 rpm for ten minutes, and the EtOH supernatant pipetted out and collected. Fresh EtOH was used to re-suspend the nanoparticles and centrifugation/EtOH supernatant collection was repeated an additional 3 times to thoroughly wash away unconjugated **NHS-FlexLP**. Supernatant washes were collected and used to estimate the weight percentage of flexLP label conjugated to the nanoparticles through UV/vis absorption studies. The fluorescently labelled nanoparticles were dried under reduced pressure to afford a free-flowing light-yellow powder.

NP FlexLP control

A similar procedure as for the **NP-FlexLP** samples was followed using unfunctionalized mesoporous silica nanoparticles (synthesized according to previous literature methods)[4] (**NP**, 40 mg) and **NHS-FlexLP** (4.0 mg). The nanoparticle powder was collected as a free-flowing white powder after washing with EtOH 3 times and collecting by centrifugation.

Structural characterization techniques

Solution-state ^{1}H and ^{13}C NMR experiments were carried out on a Bruker Avance 400MHz instrument at room temperature, and peak shifts referenced with residual solvent peaks. Infrared spectroscopy was performed on an attenuated total reflection (ATR) crystal using a PerkinElmer Frontier FT-IR spectrometer on dry sample. Thermogravimetric analysis (TGA) was performed on a Pyris 6 TGA instrument, using a platinum crucible loaded with 4-5 mg of sample. Measurements were performed under a synthetic air atmosphere (20 mL/min flow) with increasing temperature at a heating rate of 5 °C/min from 25 to 700 °C. Weight % loading of fluorophore was calculated by first assuming 100% loss of propyl-amine from **NP-NH₂** sample when heated to 700 °C, and converting weight % loss of propyl-amine functional group to moles of total propyl-amine on 1 mg of **NP** sample. This value could be used to calculate the free propyl-amine functional groups (**Table S1** column 4) and the propyl-amine groups reacted with **NHS-FlexLP** for each **NP-FlexLP** sample, to obtain the weight % loss of propyl-amide-FlexLP fluorophore (**Table S1** column 5).

Small angle powder X-ray diffraction (pXRD) patterns of nanoparticle samples were obtained using a Bruker D8-Advance X-ray diffractometer with Cu Kα radiation at 40 mA and 40 kV, scanned from 0.5 – 10 2Θ.

Transmission electron microscopy (TEM) images were collected with a Hitachi H7600 electron microscope with an acceleration voltage of 80 kV. Samples were prepared by sonicating approximately 2 mg of nanoparticles in 0.5 mL of ethanol for 10 min.

Photophysical measurements and microscopy techniques

Absorption spectroscopy and emission spectroscopy measurements were obtained using a Varian Cary 5000 UV-Vis-NIR spectrophotometer and a Photon Technology International (PTI) QuantaMaster 50 fluorimeter fitted with double excitation monochromator and 75 W Xe arc lamp as the source, respectively.

Emission lifetime experiments were carried out on a Horiba Yvon Fluorocube TCSPC apparatus, using a 370 nm NanoLED excitation source with a pulse width of 1.2 ns, pulsing at a repetition rate of 1 MHz, and using a 399 long-pass filter between sample and detector. Lifetime data were fitted against the NanoLED source background using the DAS6 Data Analysis software package, to afford sub-nanosecond deconvoluted lifetime data. All nanoparticle samples were fitted to a triexponential function, to afford chi-square values under 1.0. Multiple trials of emission lifetime experiments at 0%, 50%, and 100% water percentage confirmed the relative amplitude (%) of lifetimes to be within ± 5 %.

pH stability studies were conducted on **NP-FlexLP-10**. Three different buffer systems were used to afford a pH range from 3.0 – 10.8. Citric acid-sodium phosphate buffer was used for pH ranges 3.0 – 5.0, potassium phosphate buffer for pH ranges 6.2 – 8.0, and carbonate-bicarbonate buffer for pH ranges 9.2 – 10.8. The solutions were prepared by dissolving the indicated salts in distilled water to achieve stock solutions with ionic strengths of 0.15 M. **NP-FlexLP-10** (0.6 mg) was dispersed in 10 mL of buffer solution of known pH by sonicating for 2 minutes before absorption, emission, and emission lifetime spectroscopy measurements were obtained to prevent settling of the nanoparticles.

Fluorescence microscopy images were collected on an Olympus IX70 inverted fluorescence microscope fitted with an Olympus DP80 dual CCD 12.5 megapixel color camera, using a 400 nm longpass filter. Images were taken with a 37 ms exposure time.

NMR Spectra

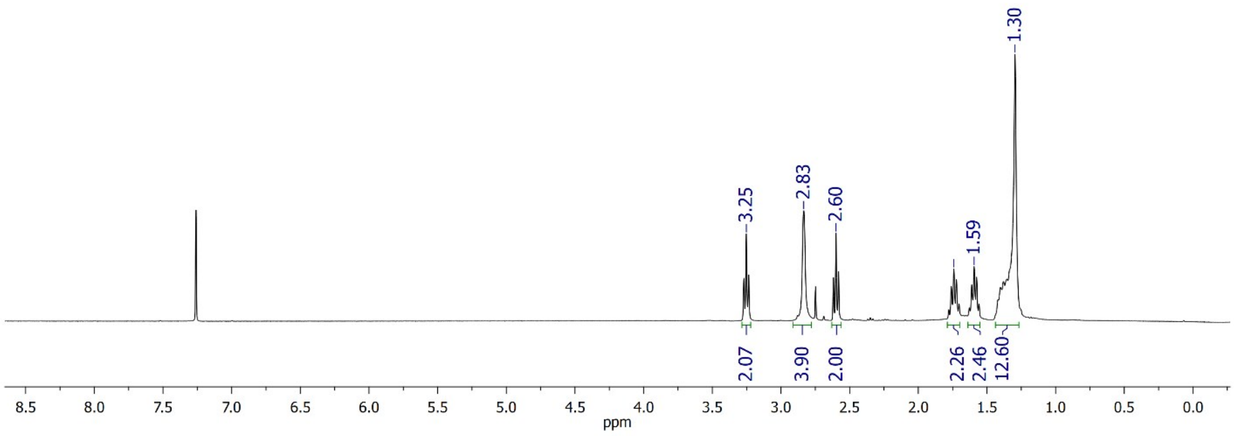

^{1}H NMR (CDCl$_3$, 400 MHz, 25 °C) **NHS-N$_3$**

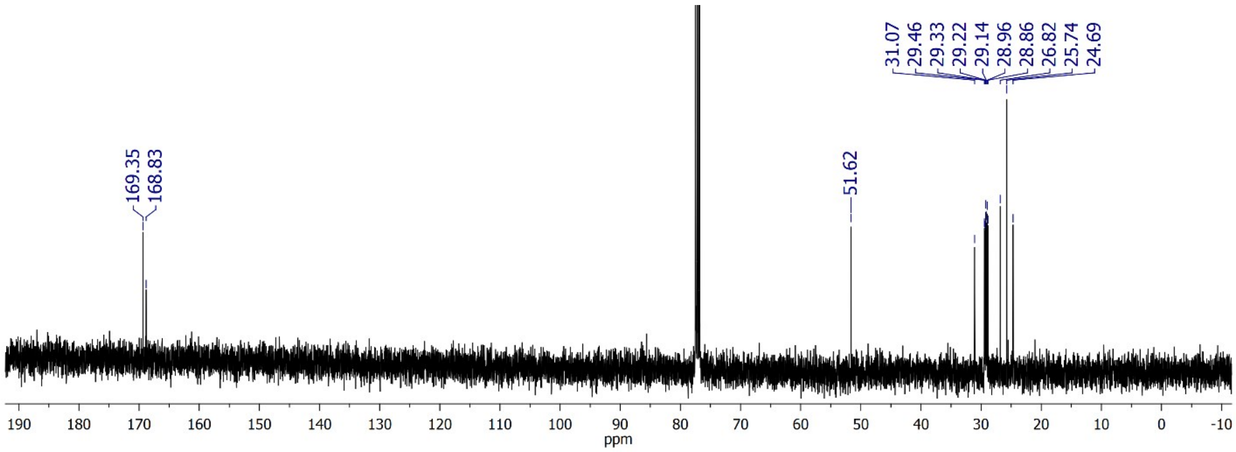

^{13}C{^{1}H} NMR (CDCl$_3$, 100 MHz, 25 °C) **NHS-N$_3$**

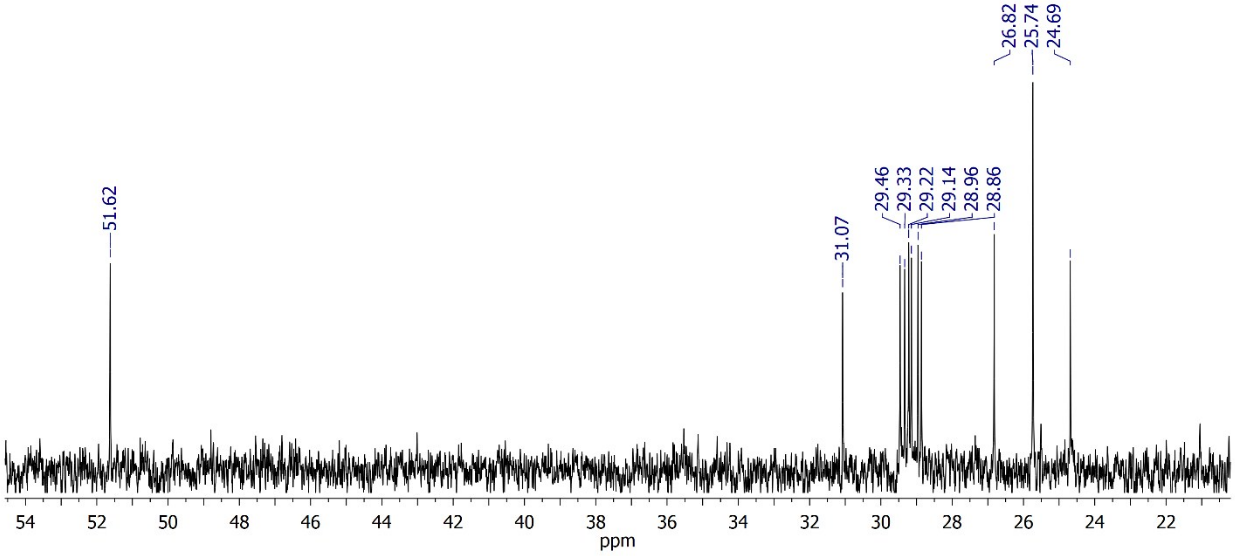

$^{13}C\{^1H\}$ NMR alkyl region ($CDCl_3$, 100 MHz, 25 °C) **NHS-N_3**

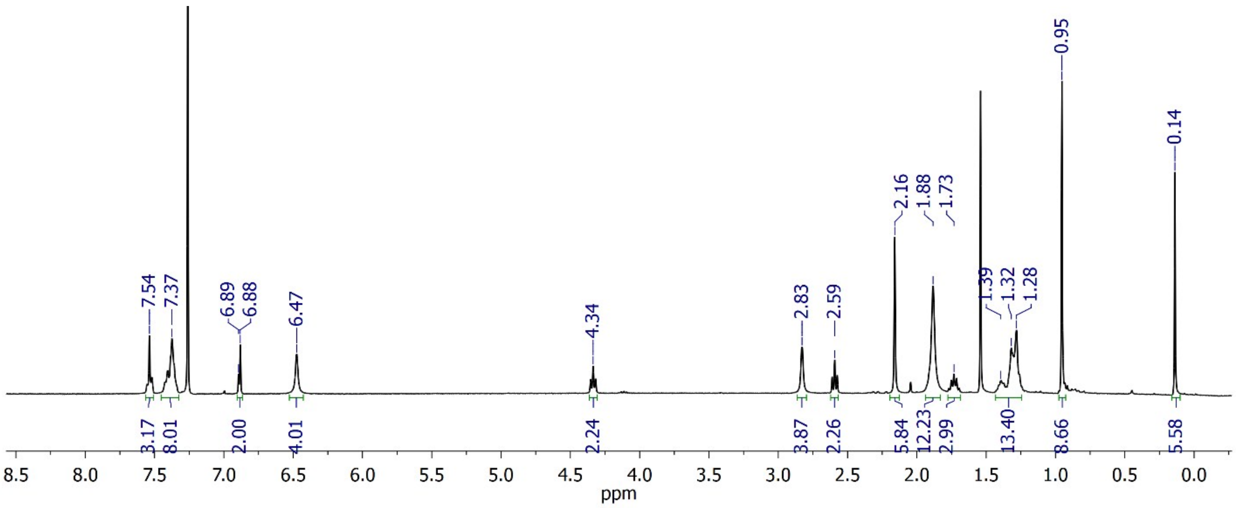

^1H NMR ($CDCl_3$, 400 MHz, 25 °C) **NHS-FlexLP**

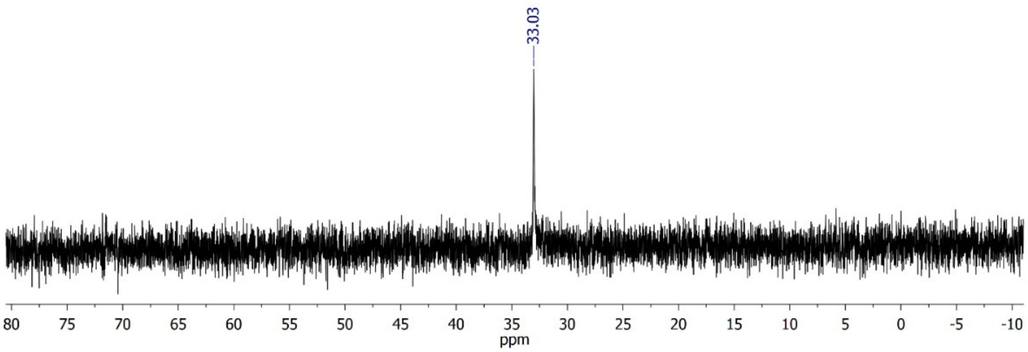

$^{31}P\{^{1}H\}$ NMR ($CDCl_3$, 162 MHz, 25 °C) **NHS-FlexLP**

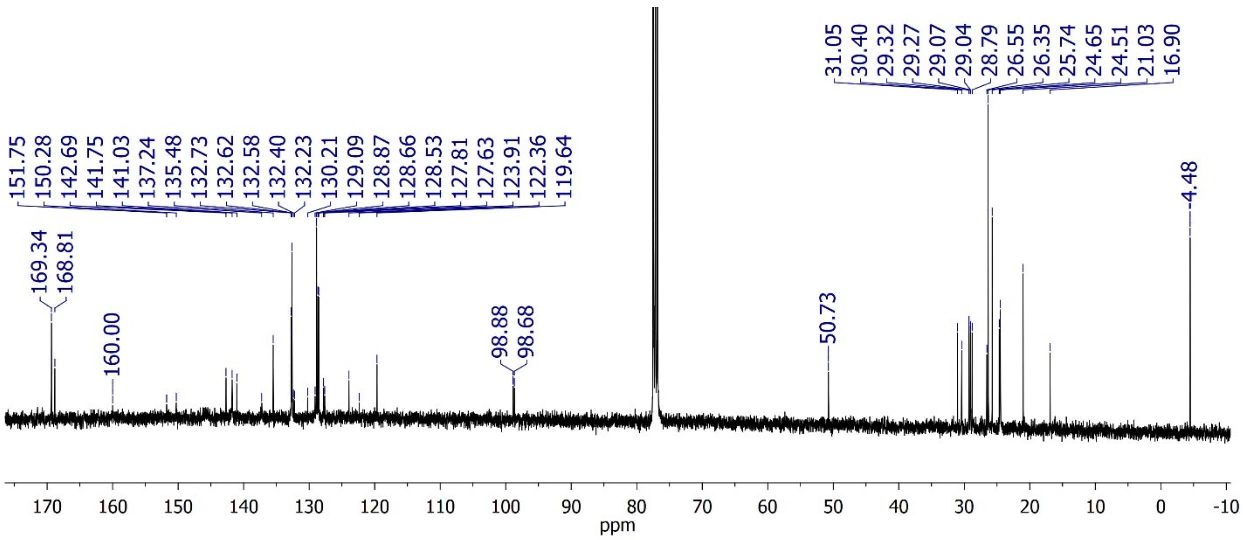

$^{13}C\{^{1}H\}$ NMR ($CDCl_3$, 100 MHz, 25 °C) **NHS-FlexLP**

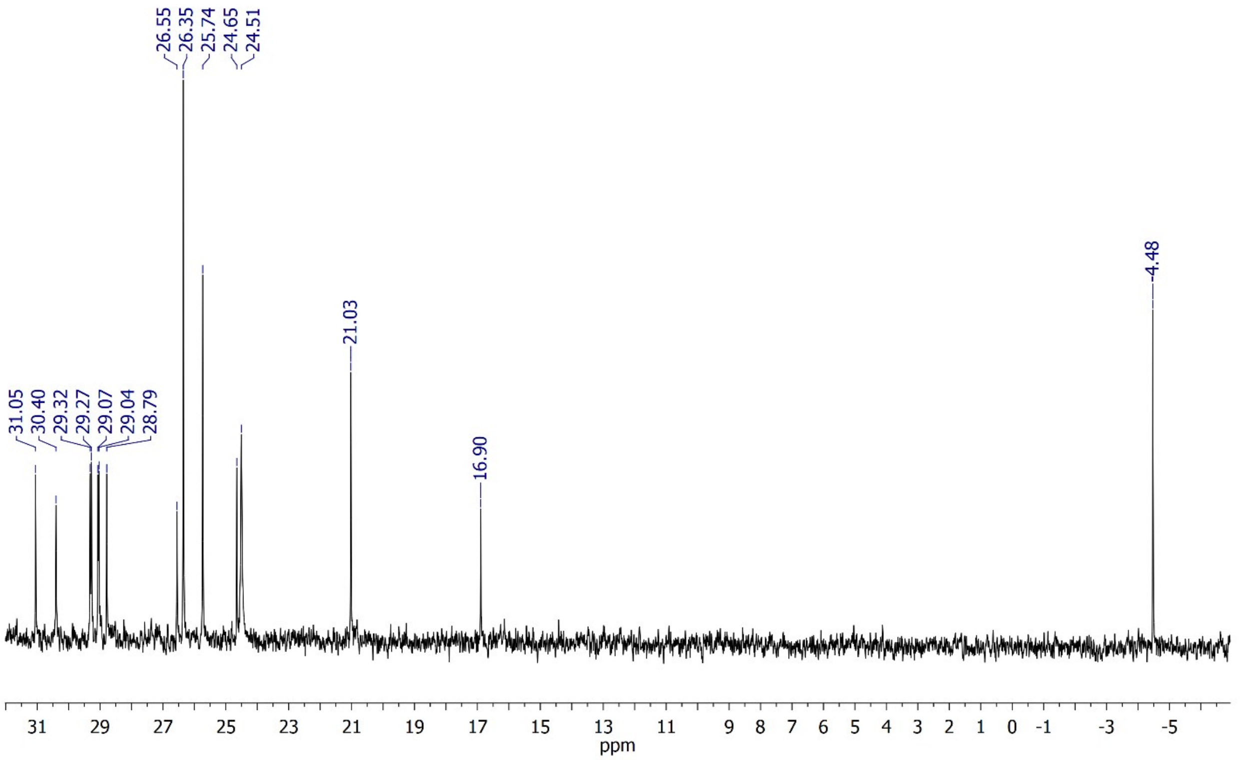

$^{13}C\{^{1}H\}$ NMR alkyl region ($CDCl_3$, 100 MHz, 25 °C) **NHS-FlexLP**

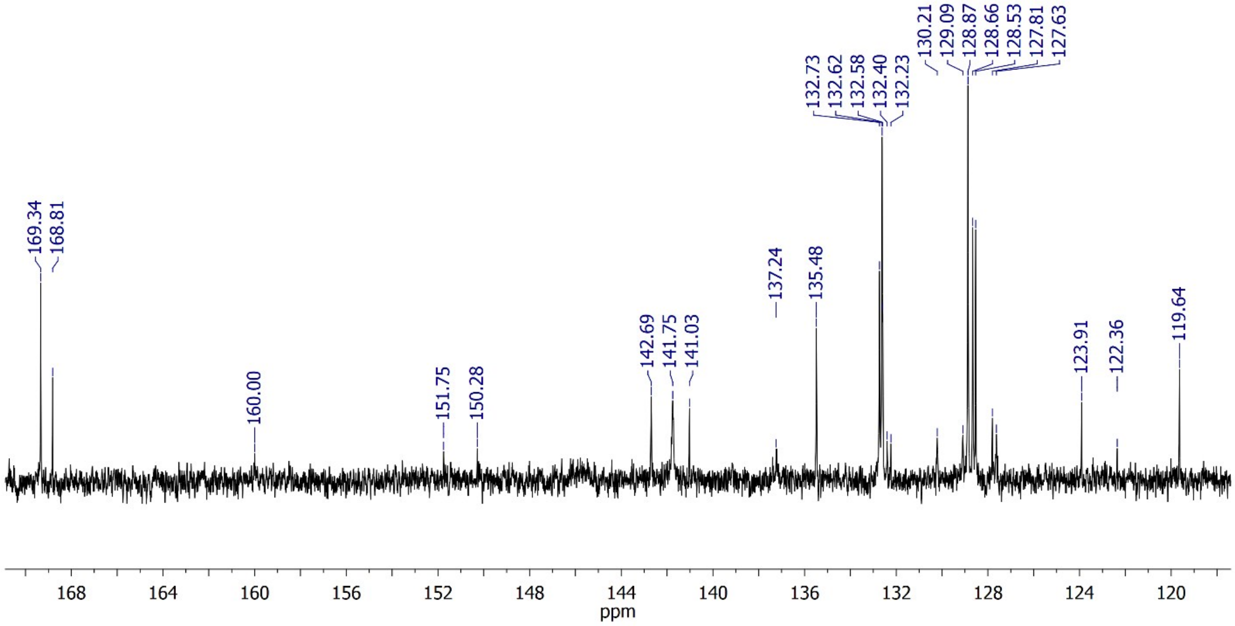

$^{13}C\{^{1}H\}$ NMR aromatic region ($CDCl_3$, 100 MHz, 25 °C) **NHS-FlexLP**

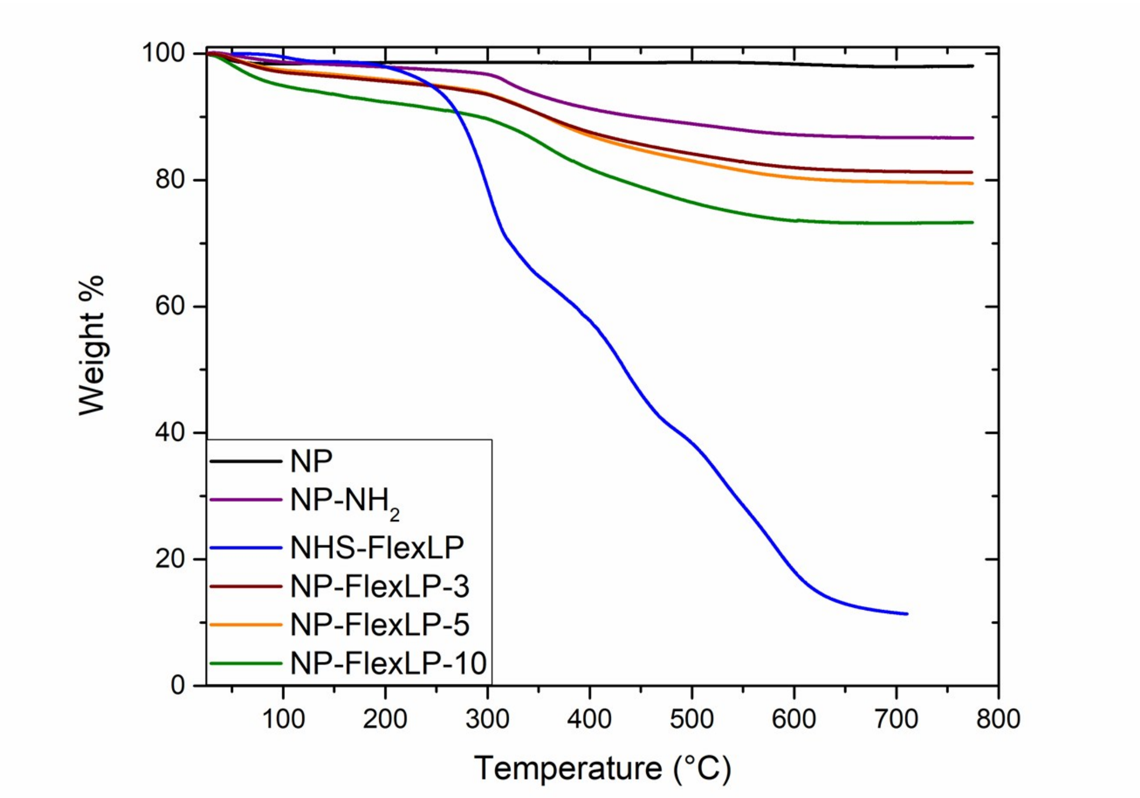

Figure S1. TGA spectra comparing weight % loss of various samples with increasing temperature.

Table S1. Weight % loading of **NHS-FlexLP** onto the nanoparticles was determined by comparing the weight % loss from TGA data.

Sample	% Weight Loss 25-100 °C	% Weight Loss 100-700 °C	Weight % Amine group	Weight Loss % FlexLP
NP	1.64	0.02	--	--
NP-NH$_2$	1.34	11.95	11.93	--
NHS-FlexLP	0.53	88.99	--	--
NP-FlexLP-3	2.96	15.69	11.70	3.96
NP-FlexLP-5	2.61	17.68	11.60	6.07
NP-FlexLP-10	5.08	21.73	11.35	10.36

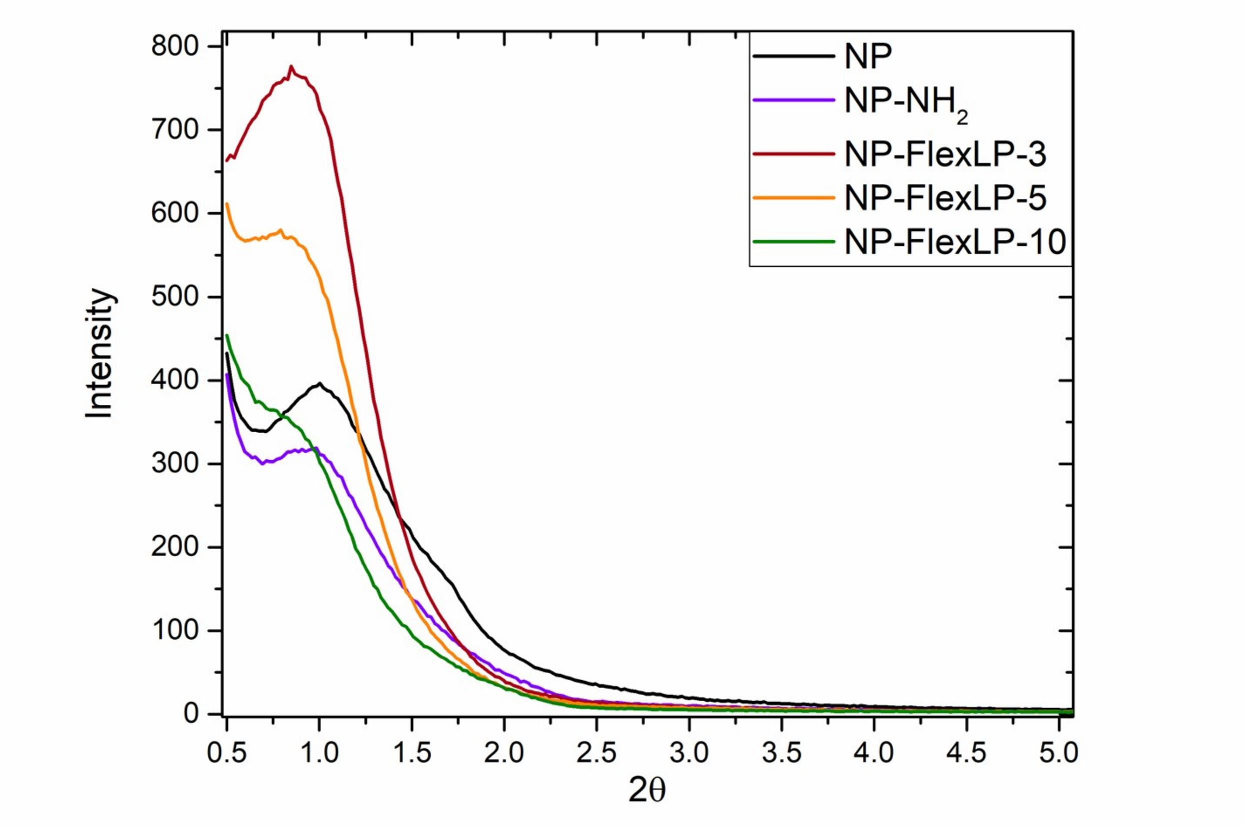

Figure S2. Small angle PXRD spectra of nanoparticle samples.

Table S2. Small angle PXRD data of mesoporous nanoparticles.

Sample	2Θ (°)	d(Å)
NP	1.0	87.4
NP-NH_2	0.98	90.1
NP-FlexLP-3	0.87	101.7
NP-FlexLP-5	0.82	107.1
NP-FlexLP-10	0.80	110.4

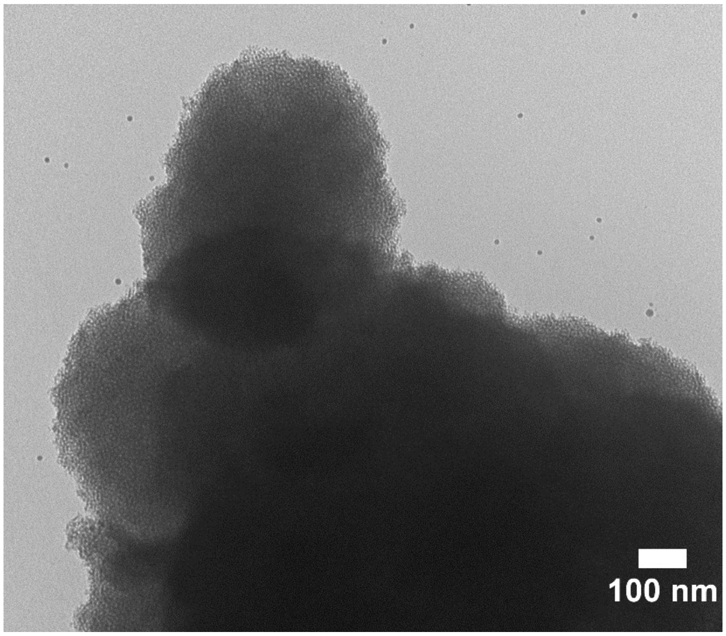

Figure S3. TEM image of unfunctionalized **NP** sample.

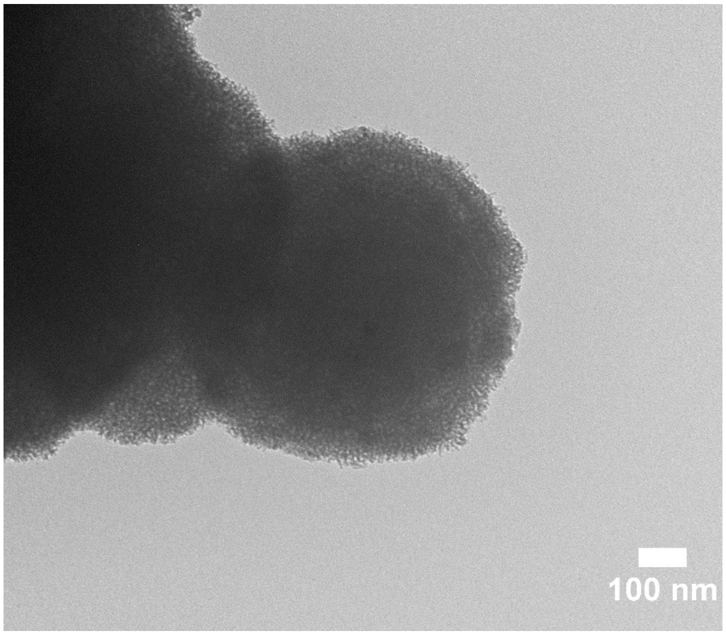

Figure S4. TEM image of **NP-NH$_2$** sample.

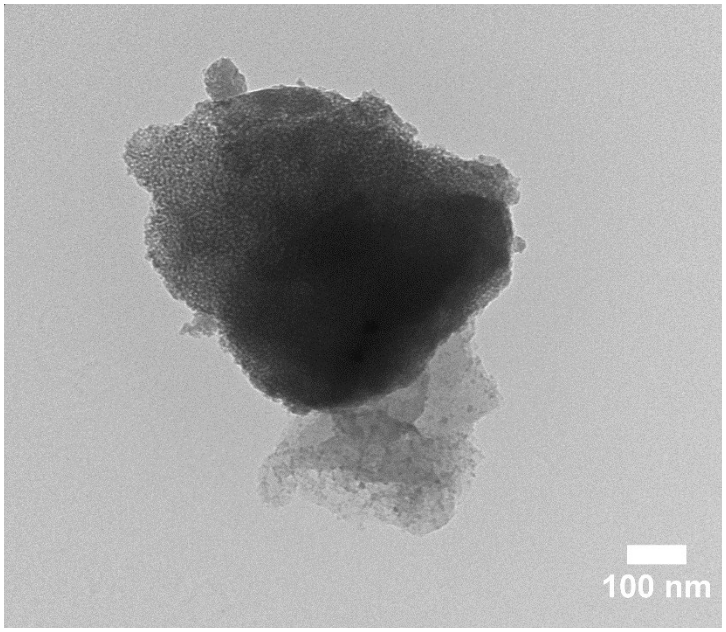

Figure S5. TEM image of **NP-FlexLP-3** sample.

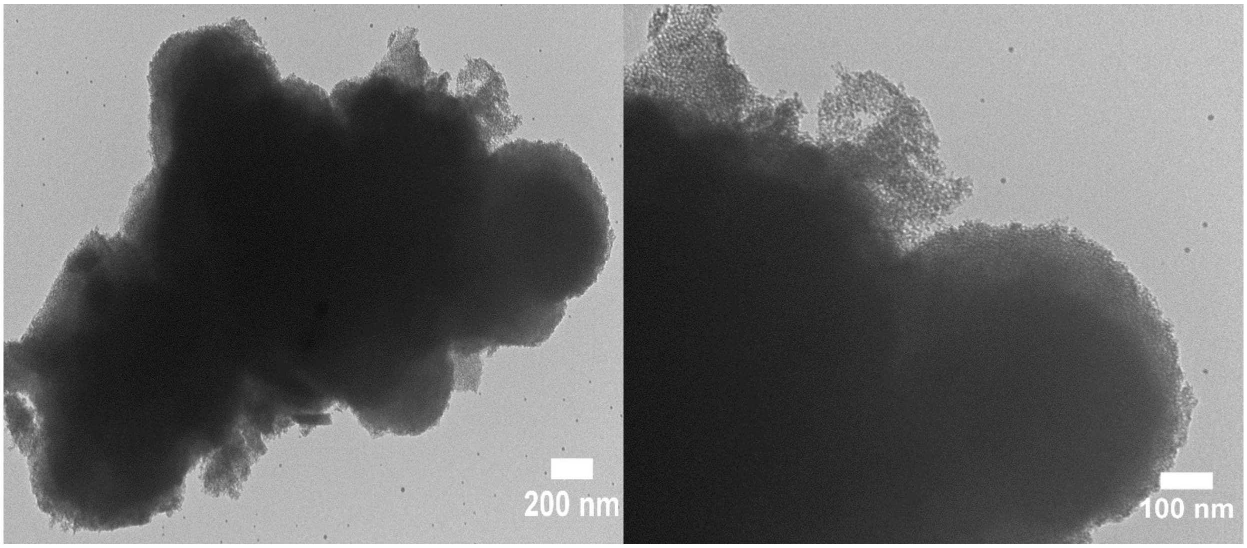

Figure S6. TEM images of **NP-FlexLP-5** sample.

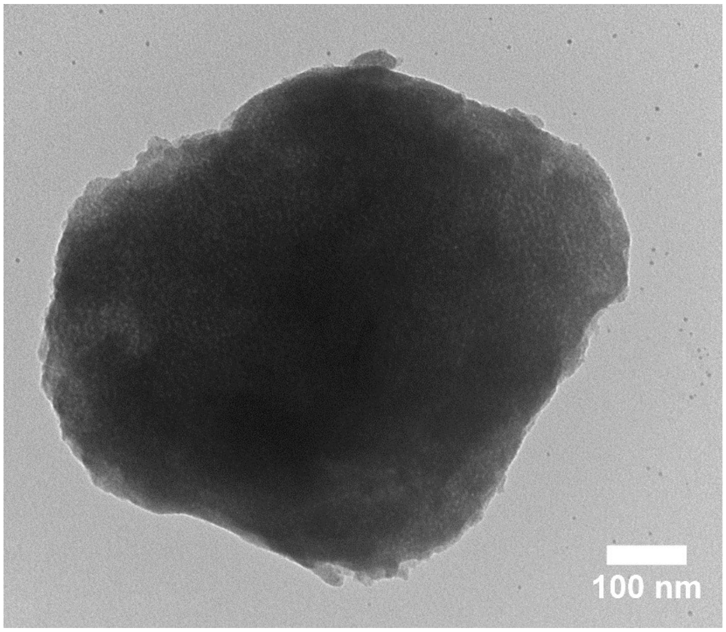

Figure S7. TEM image of **NP-FlexLP-10** sample.

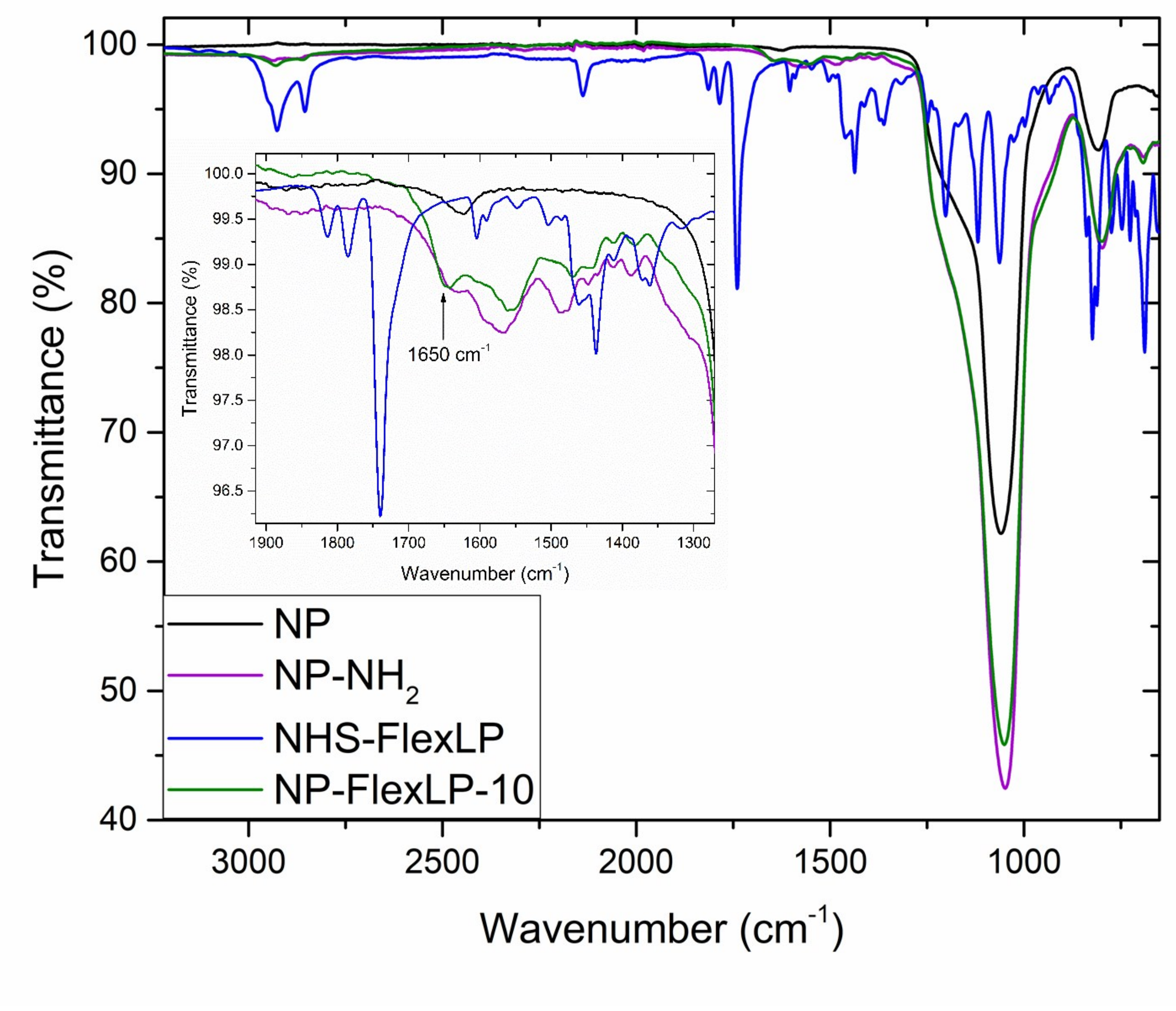

Figure S8. FTIR spectra of unfunctionalized **NP**, **NP-NH$_2$**, **NHS-FlexLP**, and **NP-FlexLP-10** samples. Inset shows a zoomed-in region highlighting the amide carbonyl C=O peak at 1650 cm^{-1} for **Np-FlexLP-10** sample. **NHS-FlexLP** trace intensity in the insert was reduced by a factor of 5 to easily compare peak wavenumbers.

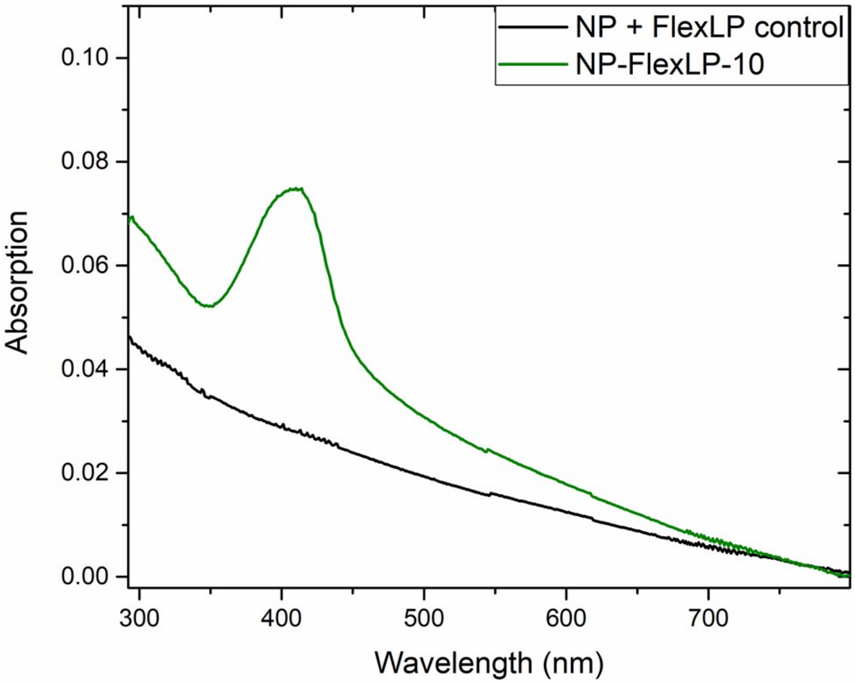

Figure S9. UV-Vis absorption spectra of **NP-FlexLP-10** (0.6 mg / 10 mL THF) and **NP+FlexLP control** sample (0.6 mg / 10 mL THF). No absorption peak at 410 nm from FlexLP is observed in the control sample.

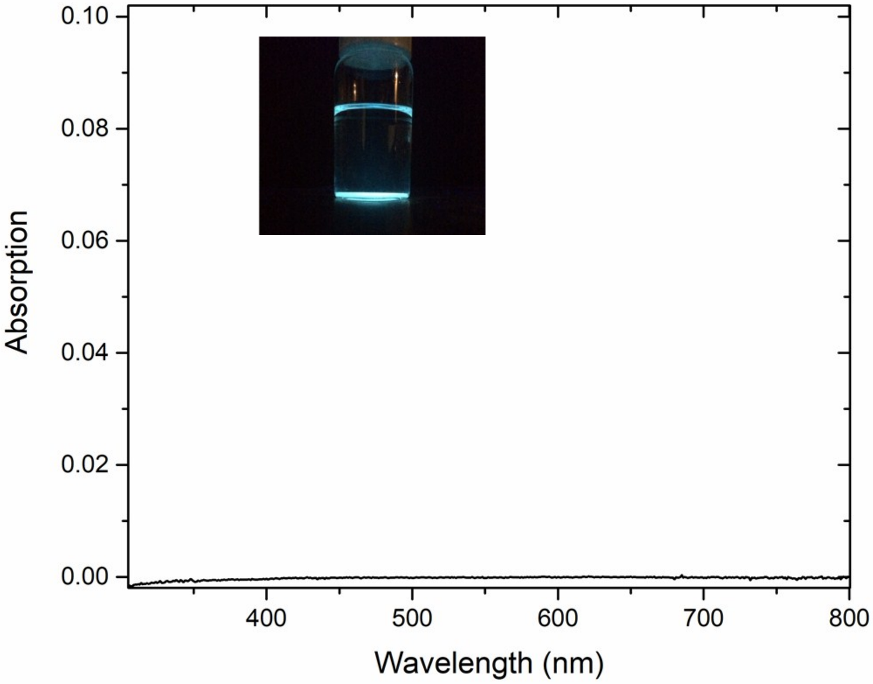

Figure S10. UV-Vis absorption spectra of FlexLP “leached” out of **NP-FlexLP-10** after 1 day in THF. Inset shows a vial of **NP-FlexLP-10** sample after 5 days in THF. Emission of the nanoparticles shows they have settled to the bottom of the vial, and no observable free FlexLP has leached into the surrounding solvent. Refracted emission can be seen at the meniscus.

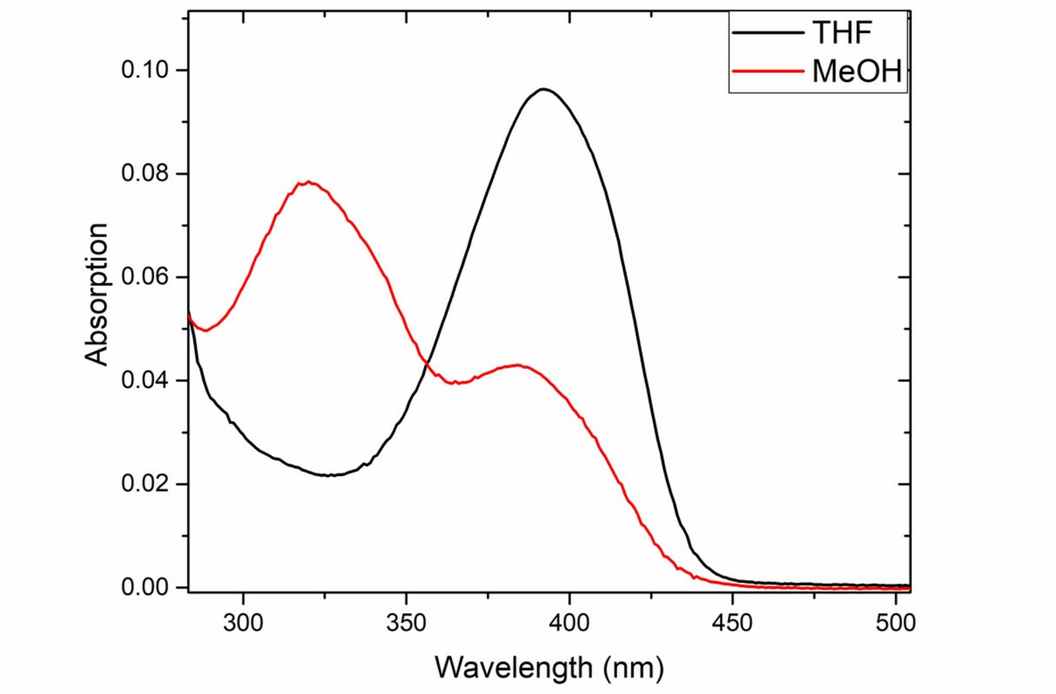

Figure S11. UV-Vis absorption spectra of **NHS-FlexLP** (4×10^{-6} M) in THF and MeOH solvent.

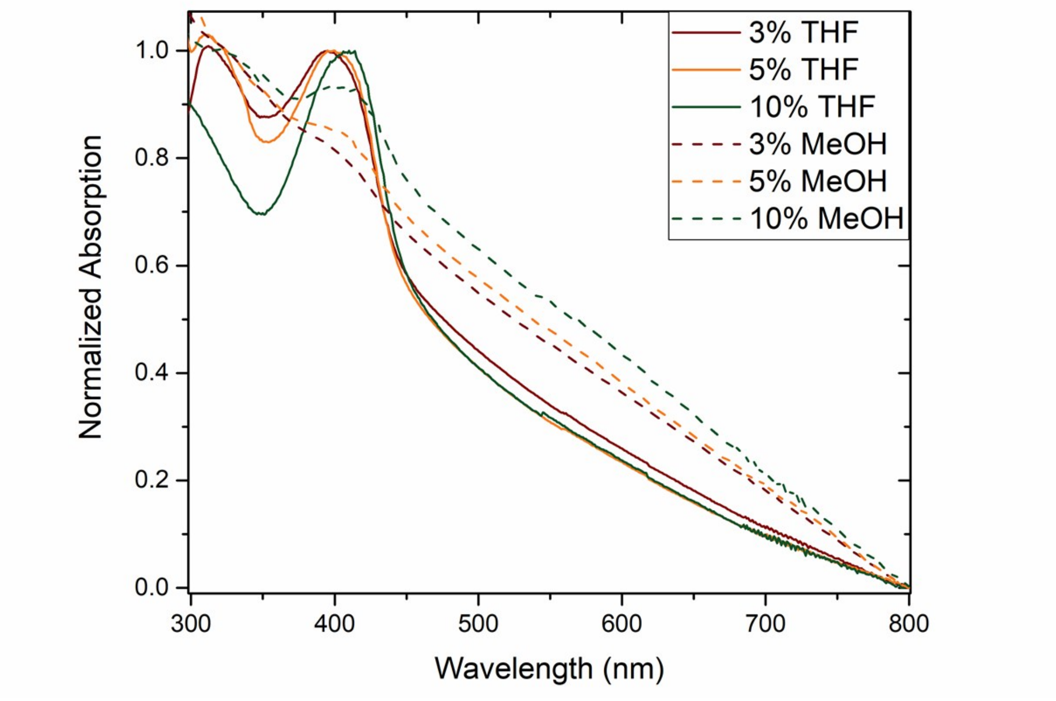

Figure S12. Normalized UV-Vis absorption spectra of **NP-FlexLP** samples (5×10^{-5} M FlexLP added) in THF (normalized at maximum peak wavelength) and MeOH (normalized at 325 nm) solvent.

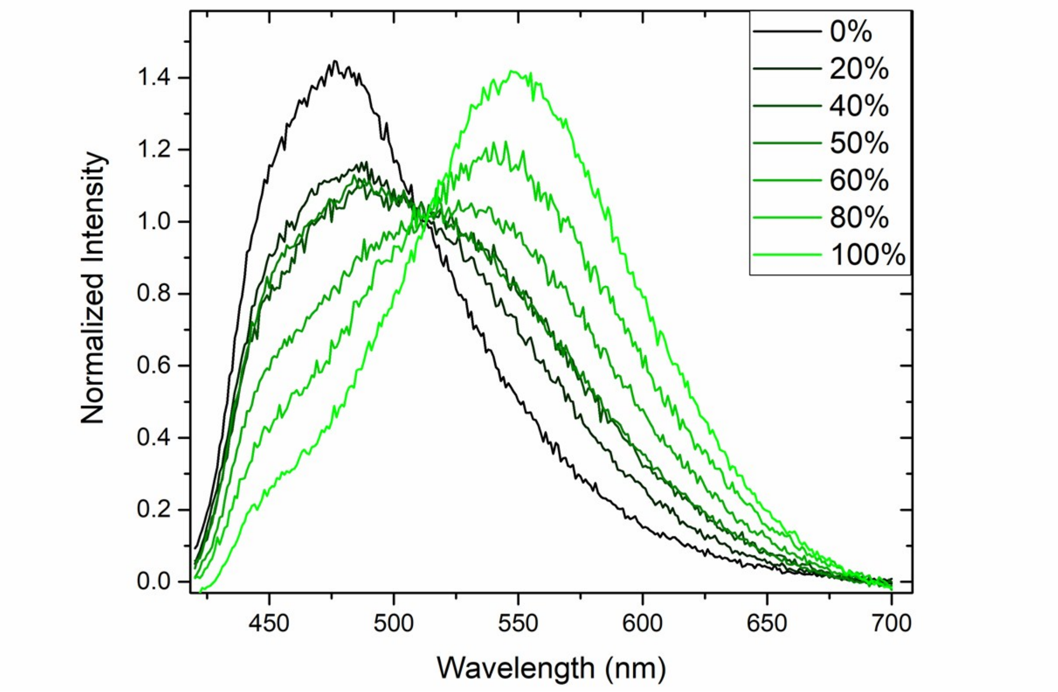

Figure S13. Emission spectra of **NP-FlexLP-3** in dioxane with increasing % by volume of water (λ_{ex} = 410 nm). Spectra were normalized at 515 nm, which is the wavelength where the emission peaks from the open and closed structure of free **NHS-FlexLP** intersect.

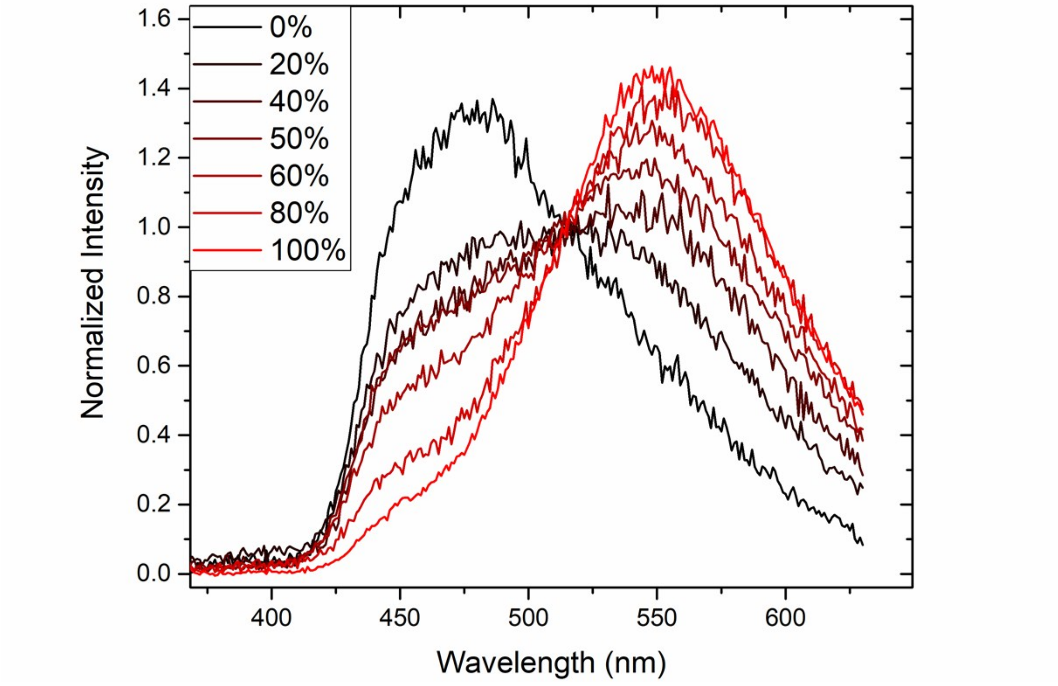

Figure S14. Emission spectra of **NP-FlexLP-3** in dioxane with increasing % by volume of water (λ_{ex} = 325 nm). Spectra were normalized at 515 nm, which is the wavelength where the emission peaks from the open and closed structure of free **NHS-FlexLP** intersect.

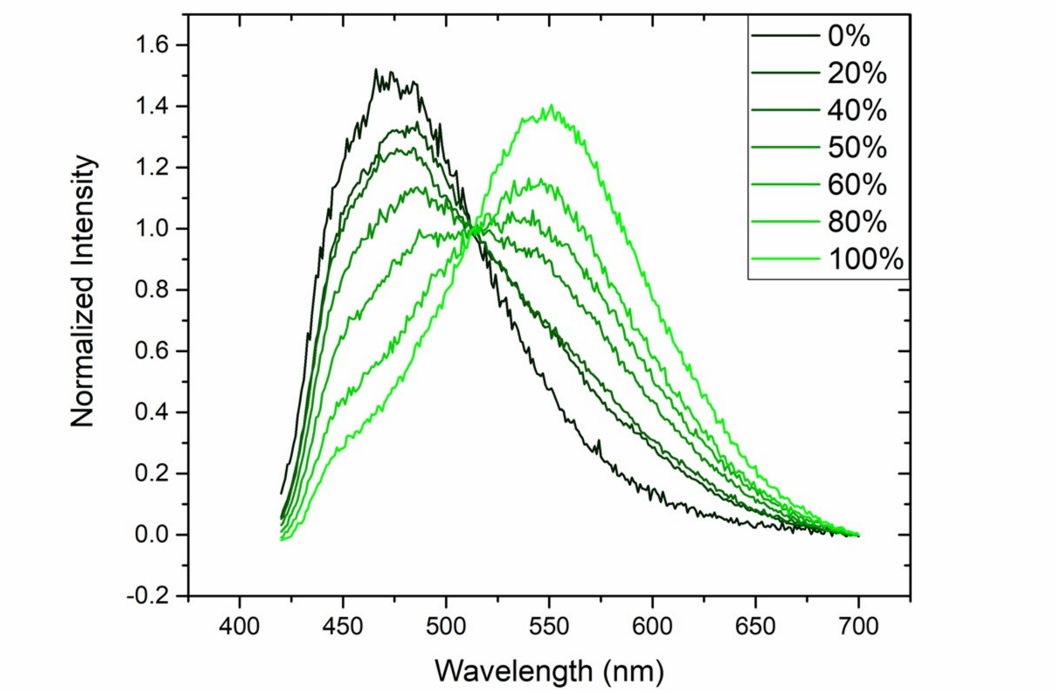

Figure S15. Emission spectra of **NP-FlexLP-5** in dioxane with increasing % by volume of water (λ_{ex} = 410 nm). Spectra were normalized at 515 nm.

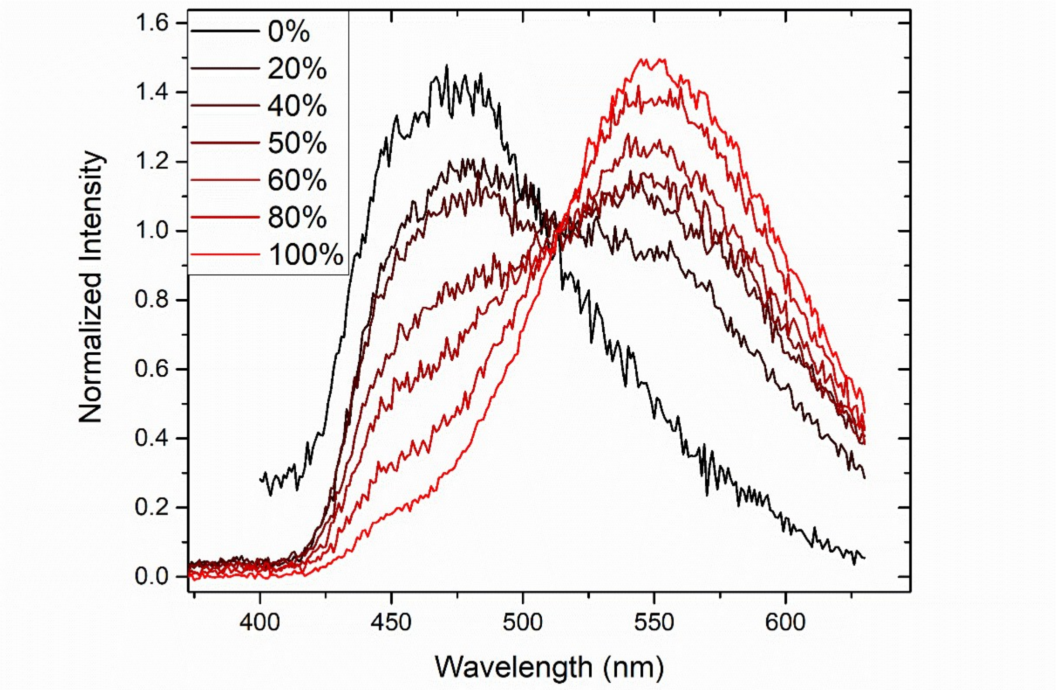

Figure S16. Emission spectra of **NP-FlexLP-5** in dioxane with increasing % by volume of water (λ_{ex} = 325 nm). Spectra were normalized at 515 nm.

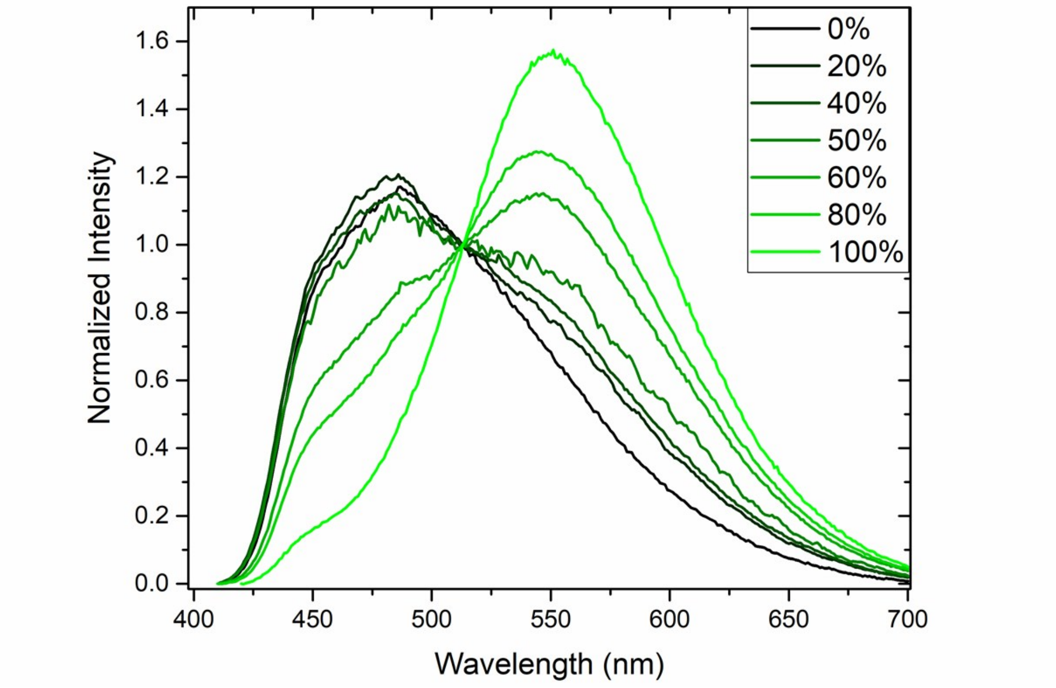

Figure S17. Emission spectra of **NP-FlexLP-10** in dioxane with increasing % by volume of water (λ_{ex} = 400 nm). Spectra were normalized at 515 nm.

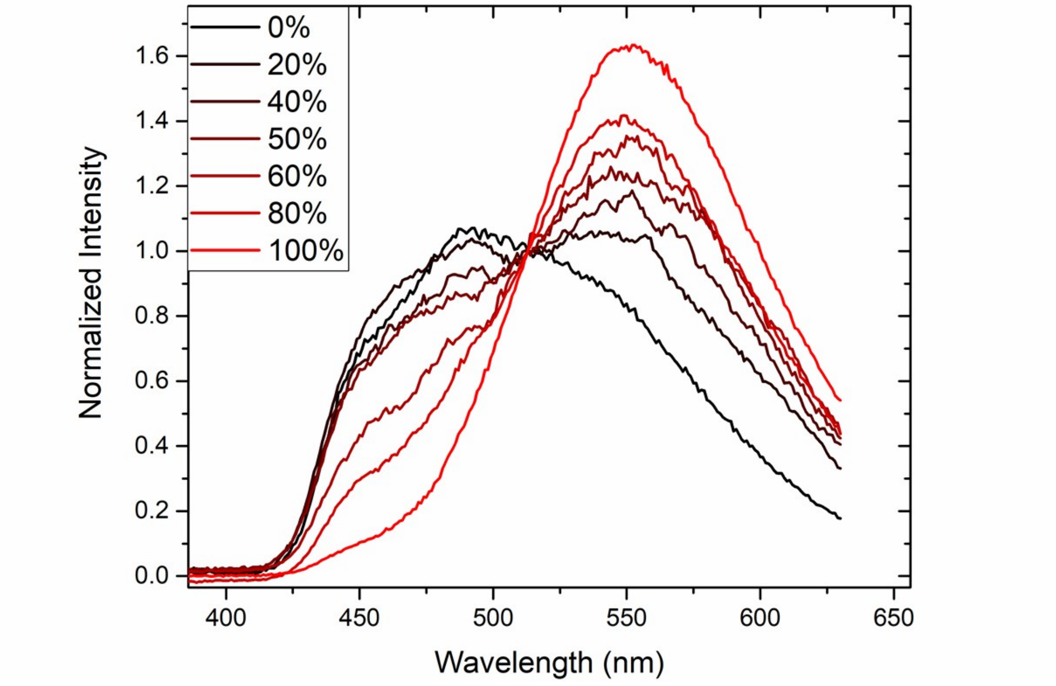

Figure S18. Emission spectra of **NP-FlexLP-10** in dioxane with increasing % by volume of water (λ_{ex} = 325 nm). Spectra were normalized at 515 nm, which is the wavelength where the emission peaks from the open and closed structure of free **NHS-FlexLP** intersect.

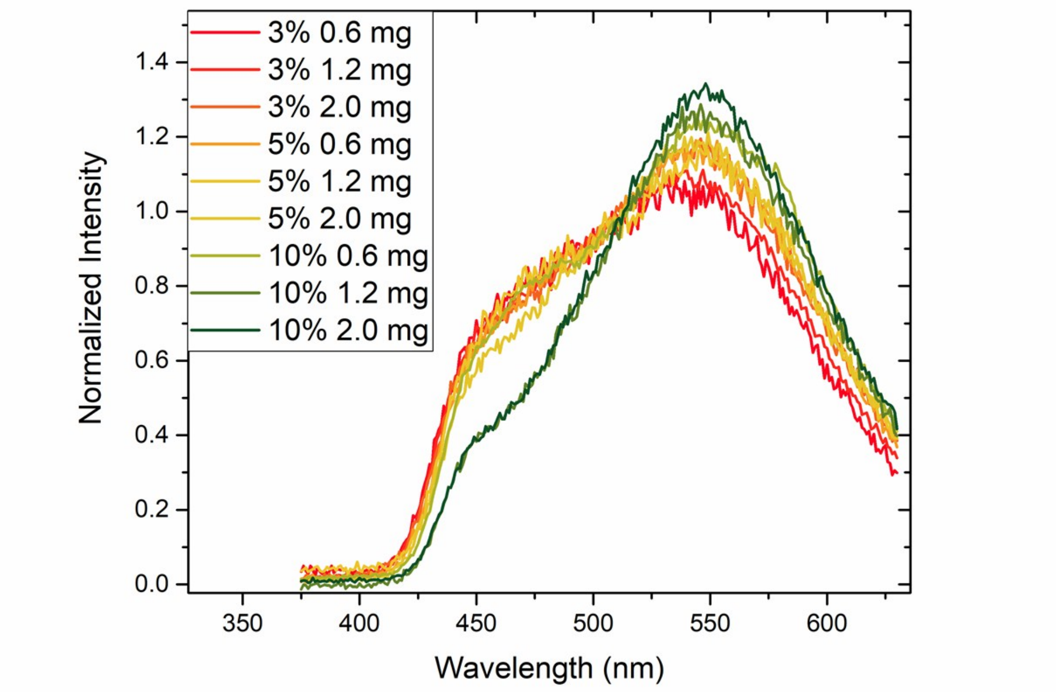

Figure S19. Emission spectra of **NP-FlexLP-3**, **-5**, and **-10** samples in 50:50 dioxane:water (v/v), with varying concentrations of sample (mg/10 mL) excited at λ_{ex} = 325 nm. Spectra were normalized at 515 nm. Variations in the ratio of open to closed form is predominantly affected by the weight percent loading of **NHS-FlexLP**, not concentration.

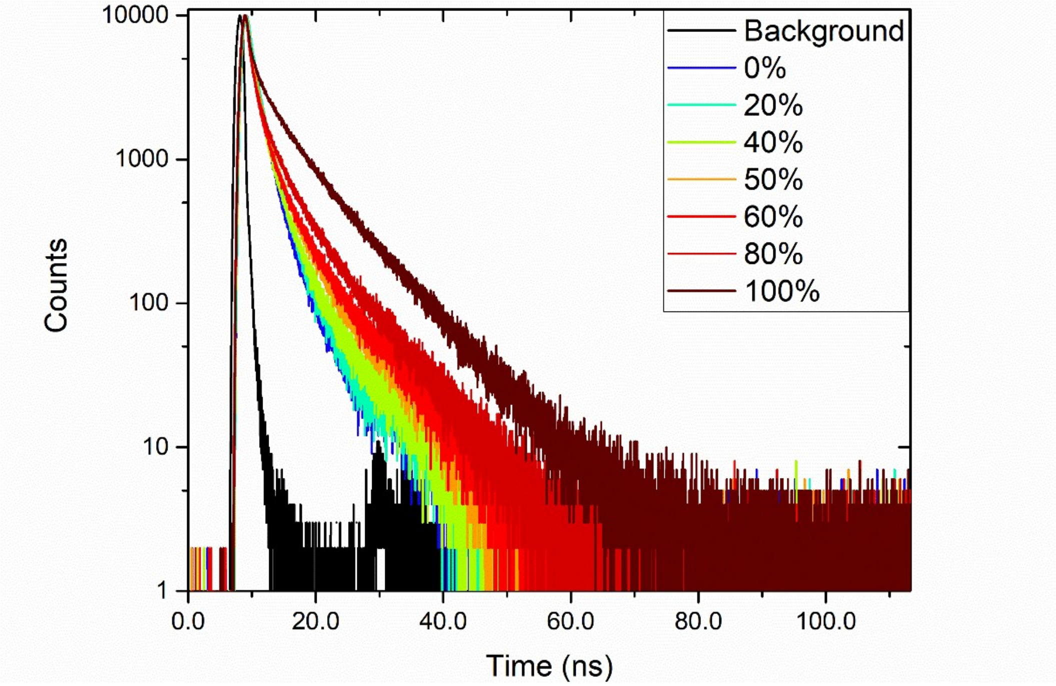

Figure S20. Emission lifetime graphs of **NP-FlexLP-3** in dioxane with increasing water content (% by volume).

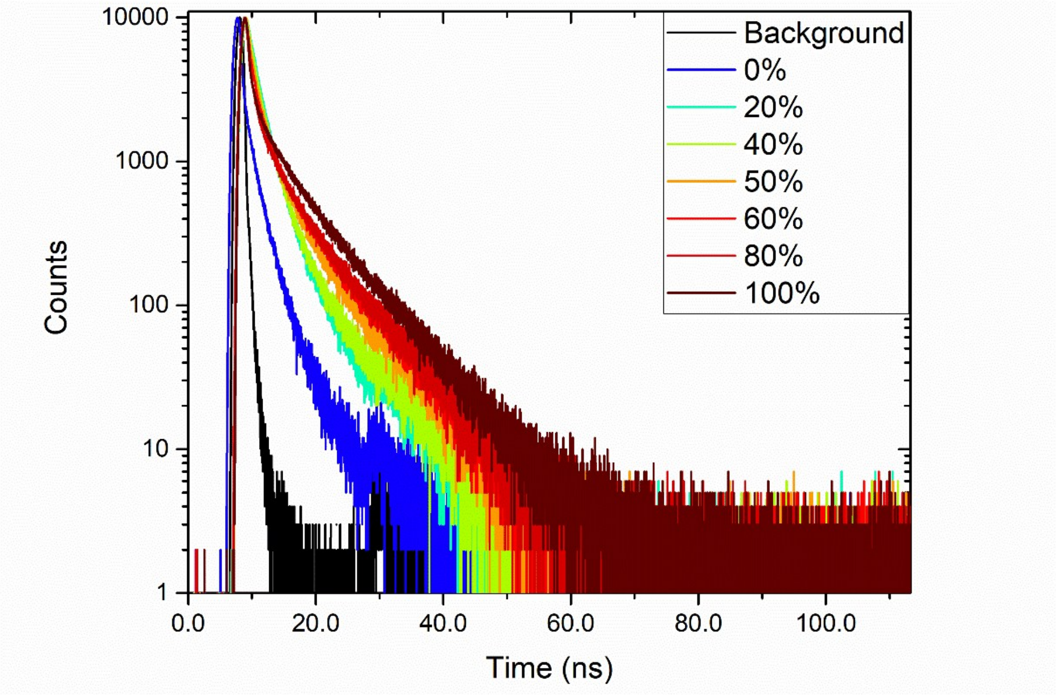

Figure S21. Emission lifetime graphs of **NP-FlexLP-5** in dioxane with increasing water content (% by volume).

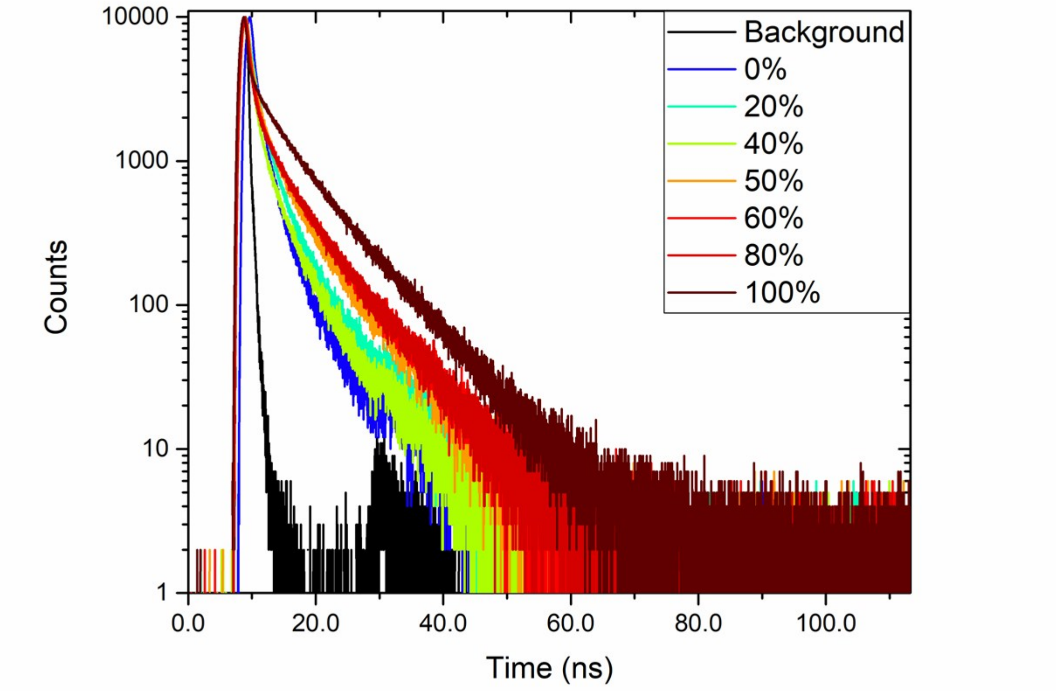

Figure S22. Emission lifetime graphs of **NP-FlexLP-10** in dioxane with increasing water content (% by volume).

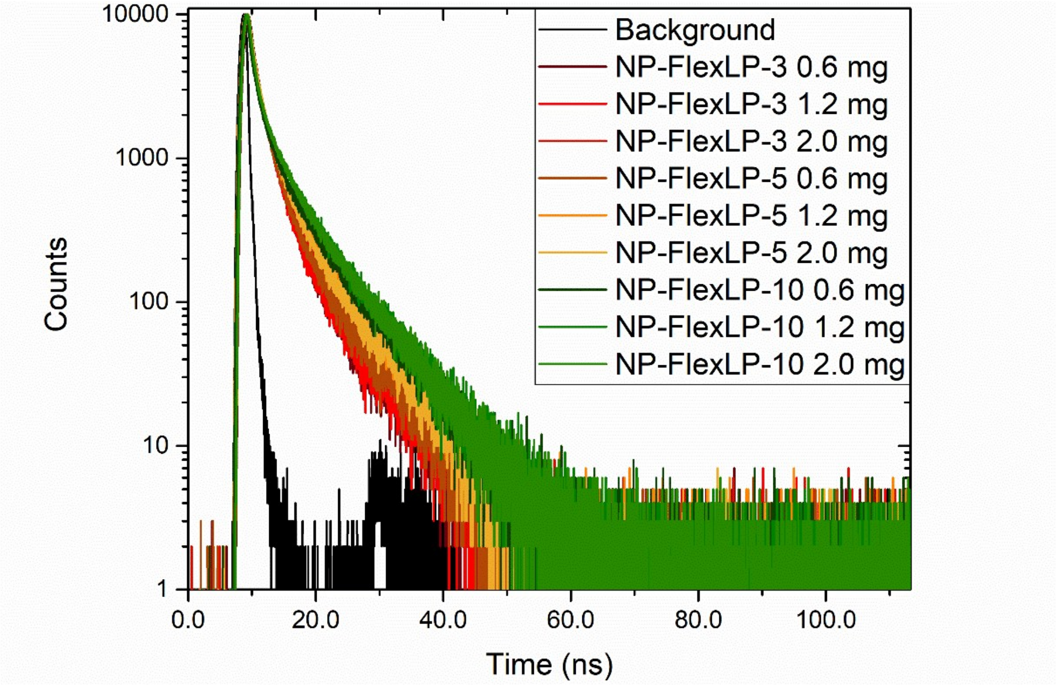

Figure S23. Emission lifetime graphs of **NP-FlexLP-3**, **-5**, and **-10** samples in 50:50 dioxane:water (v/v), with varying concentrations of sample (mg/10 mL).

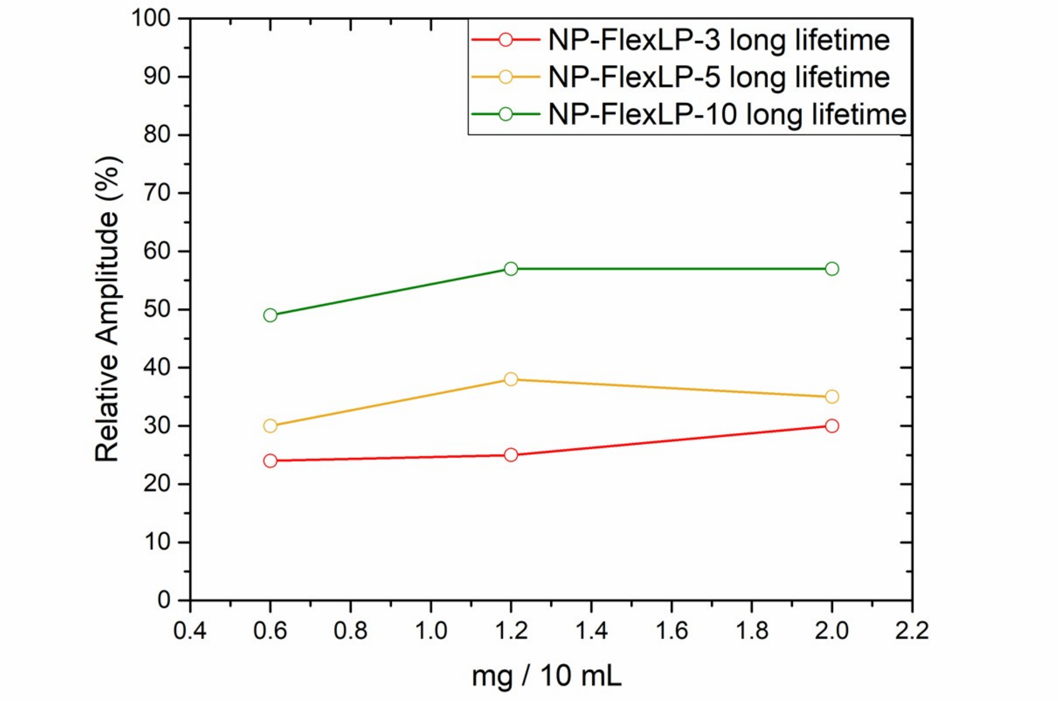

Figure S24. Relative percentages of the long emission lifetime component versus short emission lifetime component for **NP-FlexLP** samples of different concentrations in 50:50 (v/v) dioxane-water mixed solvent environments.

Table S3. Emission lifetimes (ns) and relative percentage values (% in parenthesise) for **NHS-FlexLP** and **NP-FlexLP-10** in THF and MeOH

Sample	THF			MeOH		
	<1 ns[a]	Short	Long	<1 ns[a]	Short	Long
NHS-FlexLP	--	2.25 (100)	--	--	1.90 (58.6)	7.41 (41.4)
NP-FlexLP	0.51 (9.3)	1.85 (80.1)	7.11 (10.6)	0.09 (27.9)	2.23 (13.2)	7.64 (59.0)

a. Very short lifetime is thought to be due to scattering from aggregated nanoparticles.

Table S4. Emission lifetime values (ns) and relative percentage values (% in parenthesise) of **NP-FlexLP** samples in dioxane-water mixed solvent environments.

% Water in Dioxane	**NP-FlexLP-3**			**NP-FlexLP-5**			**NP-FlexLP-10**		
	<1 ns[a]	Short	Long	<1 ns[a]	Short	Long	<1 ns[a]	Short	Long
0%	0.44 (23.5)	1.72 (64.3)	6.07 (12.2)	0.18 (54.3)	1.72 (37.3)	4.90 (8.4)	0.17 (41.2)	1.57 (44.7)	6.11 (14.1)
20%	0.45 (22.3)	1.83 (64.6)	5.84 (13.2)	0.33 (15.0)	1.88 (69.3)	6.17 (15.8)	0.32 (26.3)	1.73 (50.4)	6.25 (23.3)
40%	0.41 (28.5)	1.74 (51.8)	5.70 (19.7)	0.31 (20.0)	1.85 (60.9)	6.33 (19.1)	0.19 (38.8)	1.55 (37.2)	5.68 (24.1)
50%	0.42 (25.6)	1.90 (51.8)	6.73 (22.6)	0.32 (25.1)	1.89 (46.6)	7.07 (28.4)	0.28 (28.3)	1.73 (36.4)	7.02 (35.3)
60%	0.33 (31.5)	1.87 (40.6)	6.89 (27.9)	0.27 (28.5)	1.79 (35.7)	7.25 (35.9)	0.24 (31.7)	1.59 (25.1)	7.14 (43.2)
80%	0.29 (27.9)	1.99 (35.3)	7.13 (36.8)	0.17 (35.0)	1.72 (24.8)	7.37 (40.3)	0.20 (35.7)	1.78 (20.2)	7.24 (44.2)
100%	0.30 (18.2)	2.60 (22.4)	8.41 (59.4)	0.11 (35.2)	2.13 (16.9)	7.94 (47.9)	0.15 (24.5)	2.99 (17.6)	8.29 (57.9)

a. Very short lifetime is thought to be due to scattering from aggregated nanoparticles.

Table S5. Emission lifetime values (ns) and relative percentage values (% in parenthesis) of **NP-FlexLP** samples at three different concentrations in 50:50 dioxane-water mixed solvent environment.

Concentration (mg / 10 mL)	**NP-FlexLP-3**			**NP-FlexLP-5**			**NP-FlexLP-10**		
	<1 ns[a]	Short	Long	<1 ns[a]	Short	Long	<1 ns[a]	Short	Long
0.6	0.45 (28.3)	1.82 (54.5)	5.99 (17.2)	0.37 (26.3)	1.71 (51.5)	6.11 (22.3)	0.28 (28.3)	1.73 (36.4)	7.02 (35.3)
1.2	0.40 (26.6)	1.78 (55.3)	6.00 (18.1)	0.32 (25.1)	1.89 (46.6)	7.07 (28.4)	0.39 (30.5)	1.86 (29.7)	6.86 (39.8)
2.0	0.42 (25.6)	1.90 (51.8)	6.73 (19.7)	0.44 (27.2)	1.82 (47.1)	6.62 (25.8)	0.40 (31.6)	1.94 (29.4)	6.89 (39.0)

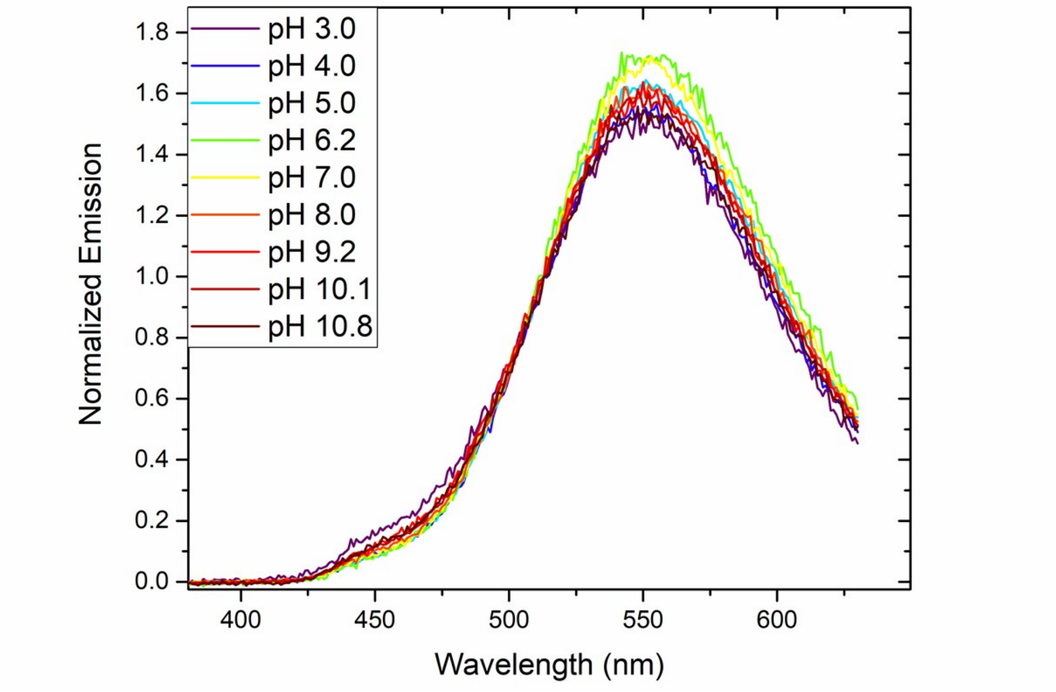

Figure S25. Normalized emission spectra (λ_{ex} = 325 nm) of **NP-FlexLP-10** in different buffer solutions of varying pH. Spectra were normalized 515 nm, the wavelength where the emission spectra of open and closed intersect.

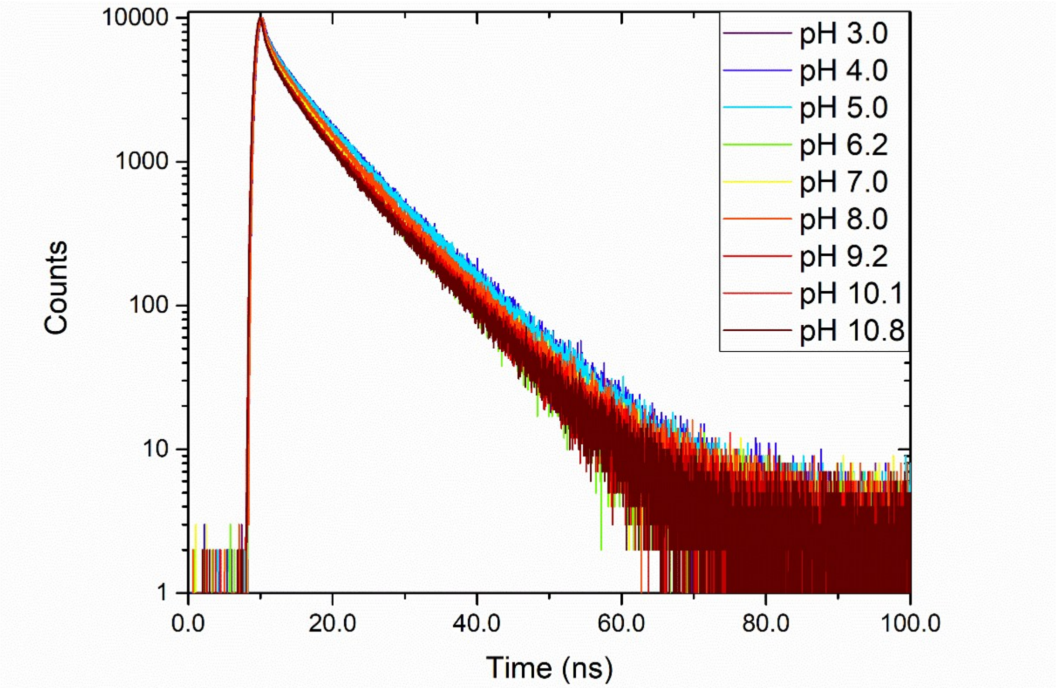

Figure S26. Emission lifetime graphs of **NP-FlexLP-10** in varying pH buffer.

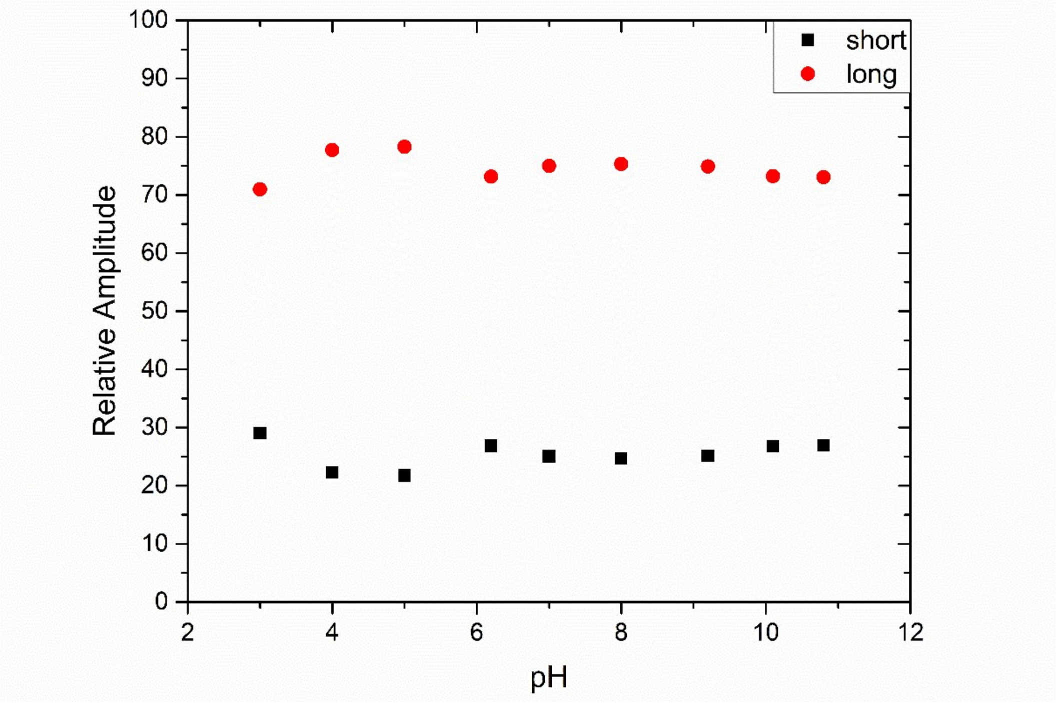

Figure S27. Relative percentage (%) of short emission lifetime and long emission lifetime of **NP-FlexLP-10** plotted against changing pH.

Table S6. Emission lifetimes (ns) and relative percentage (% in parenthesis) values of **NP-FlexLP-10** in varying pH environments.

pH	<1 ns[a] lifetime	Short lifetime	Long lifetime
3.0	0.70 (17.3)	4.07 (24.0)	8.56 (58.7)
4.0	0.31 (8.6)	3.53 (20.4)	8.56 (71.0)
5.0	0.29 (8.7)	3.44 (19.8)	8.52 (71.4)
6.2	0.23 (11.1)	3.08 (23.9)	7.83 (65.0)
7.0	0.24 (10.5)	3.15 (22.4)	8.08 (67.1)
8.0	0.26 (10.3)	3.33 (22.1)	8.24 (67.5)
9.2	0.29 (12.1)	3.11 (22.1)	8.10 (65.8)
10.1	0.29 (12.4)	3.12 (23.4)	8.06 (64.1)
10.8	0.28 (12.9)	2.99 (23.5)	8.00 (63.7)

a. Very short lifetime is thought to be due to scattering from aggregated nanoparticles.

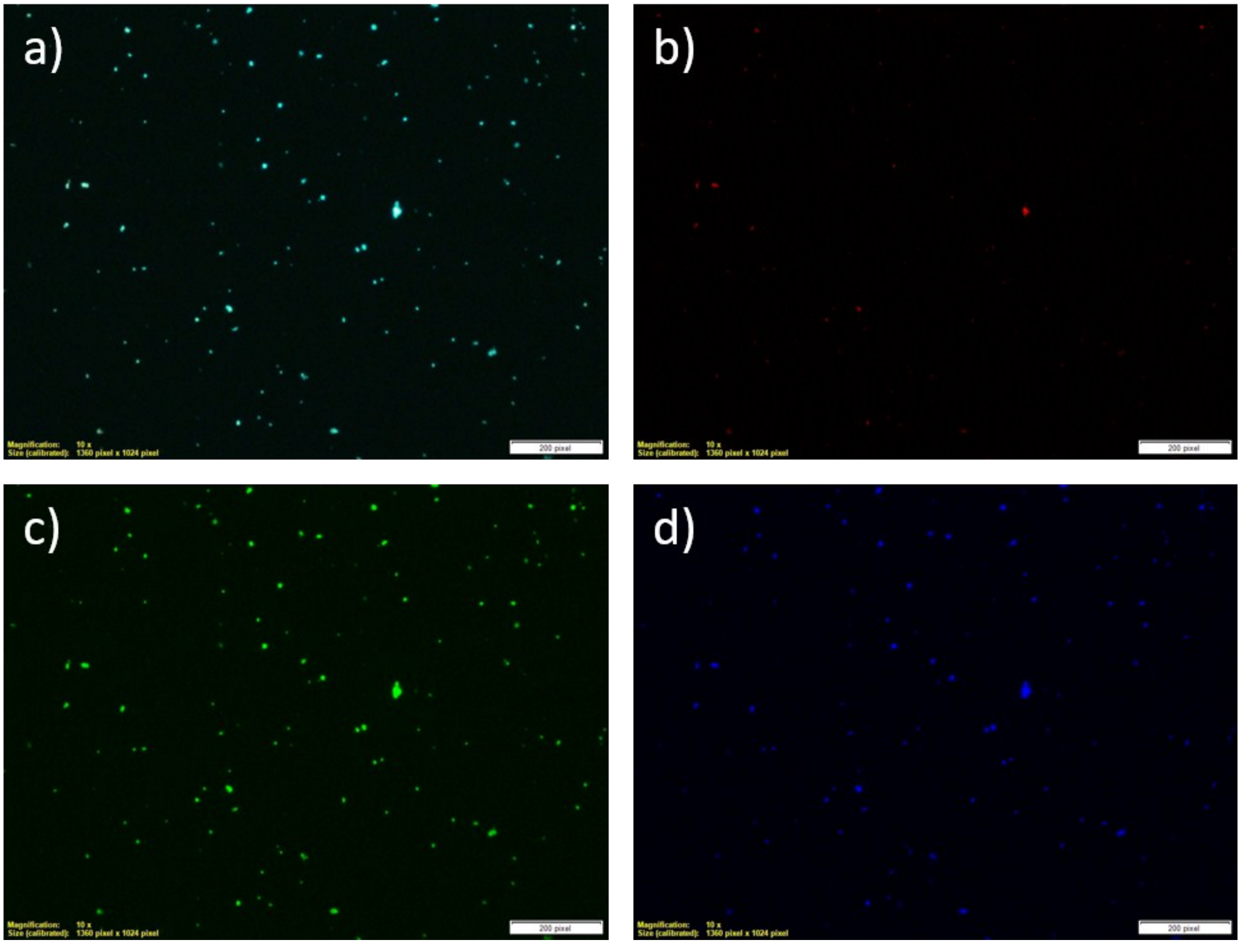

Figure S28. Fluorescence microscopy image of **NP-FlexLP-10** dispersed in dioxane (a), along with separated red (b), green (c), and blue (d) channels showing the relative emission intensity of the three channels. White scale bar = 129 µm.

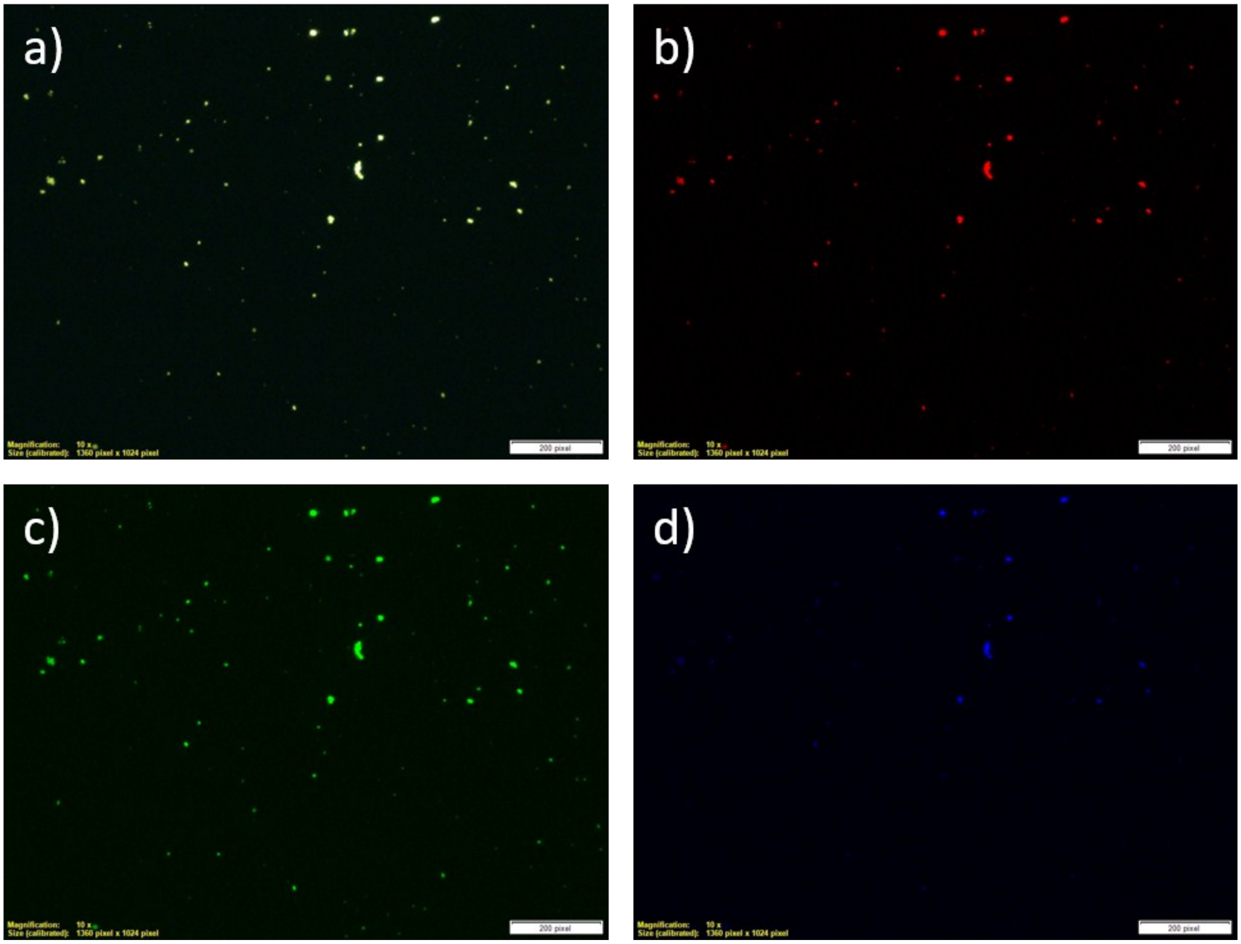

Figure S29. Fluorescence microscopy image of **NP-FlexLP-10** dispersed in water (a), along with separated red (b), green (c), and blue (d) channels showing the relative emission intensity of the three channels. White scale bar = 129 μm.

References

1. Huang, C.-W.; Wu, P.-W.; Su, W.-H.; Zhu, C.-Y.; Kuo, S.-W. *Polym. Chem.*, 2016, **7**, 795–806.
2. Arsenault, N. E.; Xu, Z.; Wolf, M. O. *Inorg. Chem*., 2019, **58**, 65-68.
3. Kotcherlakota, R.; Barui, A. K.; Prashar, S.; Fajardo, M.; Briones, D.; Rodriguez-Diéguez, A.; Patra, C. R.; Gómez-Ruiz, S. *Biomater. Sci.*, 2016, **4**, 448–459.
4. Bollu, V. S.; Barui, A. K.; Mondal, S. K., Prashar, S.; Fajardo, M.; Briones, D.; Rodriguez-Diéguez, A.; Patra, C. R.; Gómez-Ruiz, S.. *Mater. Sci. Eng. C*, 2016, **63**, 393-410.